21st Australasian Fluid Mechanics Conference
Adelaide, Australia
10-13 December 2018

Fluid–structure interaction of a flexible plate vertically fixed in a laminar boundary layer over a rigid wall

L. Wang[1], C. Lei[2] and F.-B. Tian[1]

[1]School of Engineering and Information Technology,
University of New South Wales, Canberra, ACT 2600, Australia

[2]School of Civil Engineering,
The University of Sydney, Sydney, NSW 2006, Australia

Abstract

Flow-induced vibration of a flexible structure is a common phenomenon which has recently attracted significant attention due to its fundamental and importance in engineering. Previous effort has been made to study the dynamic response of a flexible plate in uniform flows. In order to consider the interaction between a flexible plate and a wall boundary layer, this work presents a numerical study of fluid–structure interaction of a flexible plate vertically fixed in a laminar boundary layer over a rigid wall by using an immersed boundary method. The Reynolds number, structure-to-fluid mass ratio and bending rigidity have been considered. The vibrations of the plate have been discussed. Due to the interplay of the inertial, elastic and viscous forces as well as shear flow near the boundary, the plate exhibits much richer phenomena compared to flag vibrations in uniform flows. Specifically, the plate experiences steady state, periodic vibration of multiple frequencies, and chaotic vibration within the parameters considered. When the bending rigidity of the plate increases, the plate switches from periodic vibration to chaotic vibration, and then to periodic vibration.

Introduction

Flow-induced vibration of a flexible structure is a common phenomenon, such as swimming fish, flying insects and flapping flags [26]. The dynamic response of a flexible plate in flows has attracted much attention in recent years because of its fundamental and importance in engineering [29, 16, 10, 22, 23, 20, 17, 13].

Extensive experiments [9, 26, 8, 7], theoretical analyses [9, 4] and numerical simulations [29, 5, 3, 20] have studied the flow-induced vibration of a flexible plate in uniform flows, suggesting that the Reynolds number, structure-to-fluid mass ratio S, and non-dimensional bending rigidity of the plate determine the dynamic response of the flexible plate. Specifically, a lower mass ratio tends to stabilise the flexible plate-fluid system [9, 8, 7], and a massless plate in a uniform flow would maintain its equilibrium state even in the presence of large initial perturbations [29, 17]. The plate may become unstable and develop a flapping motion when the mass ratio increases [8, 7]. In addition, a larger bending rigidity tends to stabilise the system [16, 1, 8, 7, 20]. Consequently, a flexible plate with lower bending rigidity is more likely to start the vibration. Finally, a sufficiently high Reynolds number is necessary for the flow to become unstable. Recently, flow-induced vibration of multiple plates in side-by-side arrangement has been reported in Refs. [26, 14, 12, 2, 22, 23, 17]. By varying the separation between plates, in-phase, out-of-phase and erratic coupling flapping modes are observed for two plates. Additional coupling modes regarding frequency ratio between inner plate and external ones are observed for the case of three and more flexible plates [23].

More recently, Dai et al. [6] investigated the effects of a wall on the self-propelled movement of a flexible plunging plate; Lei et al. (see e.g. Refs. [25, 27, 11]) have studied the effects of a short non-metallic thin fin on heat transfer. Motivated by these two groups' work, this work studies the dynamic behaviours of a flexible plate vertically fixed in a laminar boundary layer over a rigid wall by using an immersed boundary method.

Physical Model, Mathematical Formulation and Numerical Method

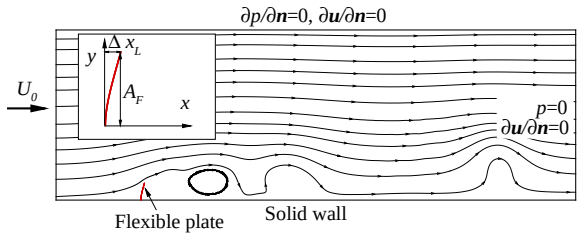

Figure 1: Schematic description of a flexible plate vertically fixed in a laminar boundary layer over a rigid wall. The inset shows the coordinate system and the tip deflection of the plate.

A flexible plate of unstretched length L vertically fixed in a laminar boundary layer over a rigid wall is considered, as shown in Fig. 1. The dynamics of the plate can be described by the following nonlinear equation [21, 24],

$$m_s \frac{\mathrm{d}^2\mathbf{X}}{\mathrm{d}t^2} = \frac{\partial}{\partial l}\left(\tau\mathbf{t} + q\mathbf{n}\right) + \mathbf{f}, \tag{1}$$

where m_s is the linear density of the plate, $\mathbf{X} = [x, y]$ is a material point on the plate, l is the arc length from the fixed point, $\mathbf{t}$ is the unit tangent vector pointing in the direction of increasing l, $\mathbf{n}$ is the unit normal vector, τ is the tension, q is the transverse stress, and $\mathbf{f}$ the hydrodynamic load. The tension and transverse stress are given by

$$\tau = E_S\left(\left|\frac{\partial\mathbf{X}}{\partial l_0}\right| - 1\right), \qquad q = \frac{\partial(E_B\kappa)}{\partial l}, \tag{2}$$

where E_S is the stretching coefficient of the plate and is large for the nearly inextensible plate, E_B is the bending modulus, κ is the local curvature, and l_0 is the arc length in the unstretched state. The boundary conditions at $l = 0$ are given by,

$$\mathbf{X} = (0, 0), \qquad \frac{\partial\mathbf{X}}{\partial l} = [0,\ 1]. \tag{3}$$

At the trailing edge, $\kappa = 0$ and $\partial\kappa/\partial l = 0$.

The flow dynamics is governed by the incompressible viscous Navier–Stokes equations,

$$\frac{\partial\mathbf{u}}{\partial t} + \nabla\cdot(\mathbf{u}\mathbf{u}) = -\frac{1}{\rho_f}\nabla p + \nu_f\nabla^2\mathbf{u}, \qquad \nabla\cdot\mathbf{u} = 0, \tag{4}$$

where $\mathbf{u}$ is the velocity, ρ_f and ν_f are respectively the fluid density and viscosity, and p is the pressure. No-slip and no-penetration conditions are specified at the surface of the plate. Other boundary conditions over the computational domain boundaries are shown in Fig. 1. To parameterize the problem, we define the non-dimensional groups including the Reynolds number, mass ratio, bending rigidity and stretching rigidity, given respectively by

$$Re = \frac{U_0 L}{\nu_f}, \quad m^* = \frac{m_s}{\rho_f L}, \quad E_B^* = \frac{E_B}{\rho_f U_0^2 L^3}, \quad E_S^* = \frac{E_S}{\rho_f U_0^2 L}. \quad (5)$$

In this work, $E_S^* = 6400$ so that the plate is nearly inextensible.

The governing equations with boundary conditions are solved by using an in-house solver. Specifically, the incompressible flow is solved using a sharp-interface immersed-boundary method with a special treatment to suppress the pressure oscillations associated with the moving boundaries [20, 21, 19, 24]. The plate is discretised by a set of Lagrangian points initially distributed uniformly along it. A standard central finite difference scheme is used to solve the structure dynamics iteratively. The fluid–structure interaction is iterated in a partitioned manner [19, 18]. The fluid-structure solver has been extensively validated and applied to a few topics [21, 19, 24, 15]. For brevity, the validations of the solver are not included in this paper.

The computational domain has a size of $30L \times 10L$. The distance from the inlet to the plate is $5L$. The entire domain consists of a nonuniform Cartesian grid of 441×207 points. The mesh contains a horizontal band of width $2L$ and a vertical band of width $1.5L$ in which the grid points are uniformly and densely distributed such that the grid spacing $\Delta x = \Delta y = 0.01L$. A total number of 101 nodes are used to discretise the plate. The time step size is $\Delta t = 0.0025L/U_0$. All simulations are carried out until periodic or continuous erratic vibrations are observed.

Results and Discussion

In this work, we consider the effects of Re (from 100 to 800), m^* (from 1.5 to 3.0) and E_B^* (from 0.1 to 1.6) on the dynamic behaviours of the flexible plate.

Effects of the Reynolds Number

Here we set $m^* = 3.0$ and $E_B^* = 0.4$ and compare the dynamics of the plate for $Re = 100$, 200, 400 and 800. Fig. 2 shows the time histories of the plate tip deflection (Δx_L in Fig. 1) and the corresponding PSD (power spectral density) which is re-scaled by the sum of all peaks. Several interesting observations can be made from this figure. First, the flow is steady and the plate is stable at the lowest Reynolds number (i.e. $Re = 100$). Second, when the Reynolds number increases, the plate vibrates and becomes erratic at large Reynolds numbers (e.g. $Re = 800$). The above two observations are similar to the case of flow-induced vibration of a flag in uniform flows reported in Ref. [5]. Third, there is no single-frequency vibration for the plate. The plate experiences sustained vibrations with a few frequencies, as indicated by the PDS of ΔX_L at $Re = 200$. This is due to the plate-vortex-boundary interaction. Finally, the mean displacement of the plate increases with the Reynolds number which is consistent with the 3D observation of a flexible plate in uniform flows in Ref. [19], but in contrast with a 2D plate in uniform flows studied by Zhu et al. [28]. The most significant difference in flow structures between the current study and Ref. [28] is that the unsteady vortex shedding occurs here, while the flow is steady in Ref. [28]. This is a reasonable explanation of the different Re-mean ΔX_L observations.

Effects of the Mass Ratio

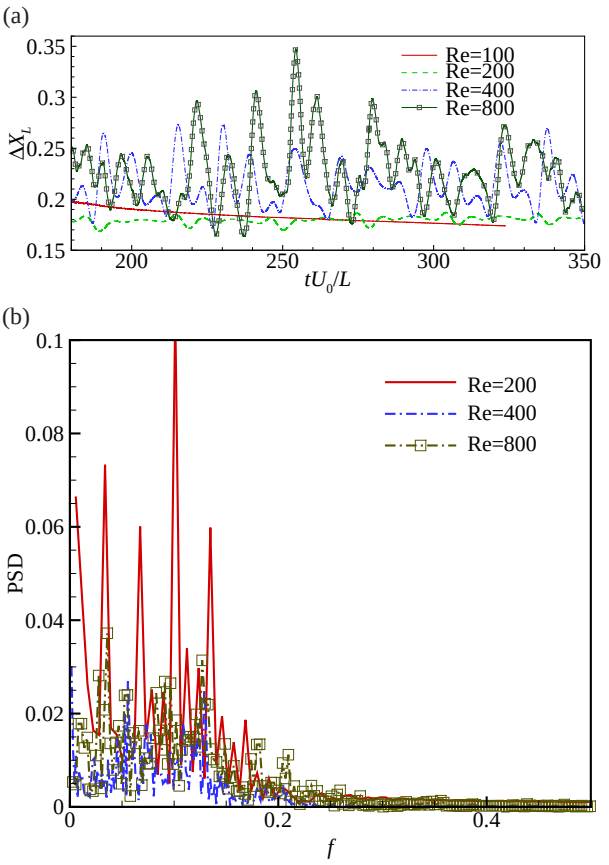

Figure 2: Re effects: (a) ΔX_L and (b) PSD.

Regarding the effect of mass ratio, simulations are conducted at $Re = 400$, $E_B^* = 0.4$ and $m^* = 1.5$, 3.0 and 6.0. The time histories of the plate tip displacement and the corresponding PSD are presented in Fig. 3. For low mass ratio (e.g. $m^* = 1.5$), the plate undergoes vibration with a few discrete frequencies. The vibration becomes chaotic when the mass ratio increases. This observation is similar to the flow-induced vibration of a flag in uniform flows [5].

Effects of the Bending Rigidity

Finally, we consider the effect of the bending rigidity. Here the computational parameters are $Re = 400$, $m^* = 3.0$ and $E_B^* = 0.1 - 1.6$. The time histories of the plate tip displacement and the corresponding PSD are shown in Fig. 4. When E_B^* is varied from 0.1 to 1.6, the plate first undergoes vibration at discrete frequencies (e.g. $E_B^* = 0.1$), then chaotic vibration (e.g. $E_B^* = 0.2$ and 0.4) and finally vibration at discrete frequencies again (e.g. $E_B^* = 0.8$ and 1.6). This observation is different from that in flag flapping where large E_B^* stabilises the flow. This may be explained by the effective Reynolds number and vortex-wall interaction. For small bending rigidity, the deformation of the plate is large, and thus the front area (see A_F in Fig. 1) is small. Consequently, the effective Reynolds number is small, leading to a vibration at discrete frequencies. When the bending rigidity increases, the effective Reynolds number increases, leading to chaotic vibration. If we further increase the bending rigidity, the coupled vibration is stabilised.

To further discuss the frequency properties, the frequencies of $E_B^* = 0.1$, 0.8 and 1.6 are shown in Fig. 5. In this figure, $f_{0.1}$, $f_{0.8}$ and $f_{1.6}$ are respectively the fundamental frequencies for $E_B^* = 0.1$, 0.8 and 1.6 which are very close to their first eigenfrequency. For all the three cases, the frequencies can be explained by $n \times f_{0.1,0.8 \text{or} 1.6}/N$ where $N = 1$ for $E_B^* = 0.1$, $N = 2$

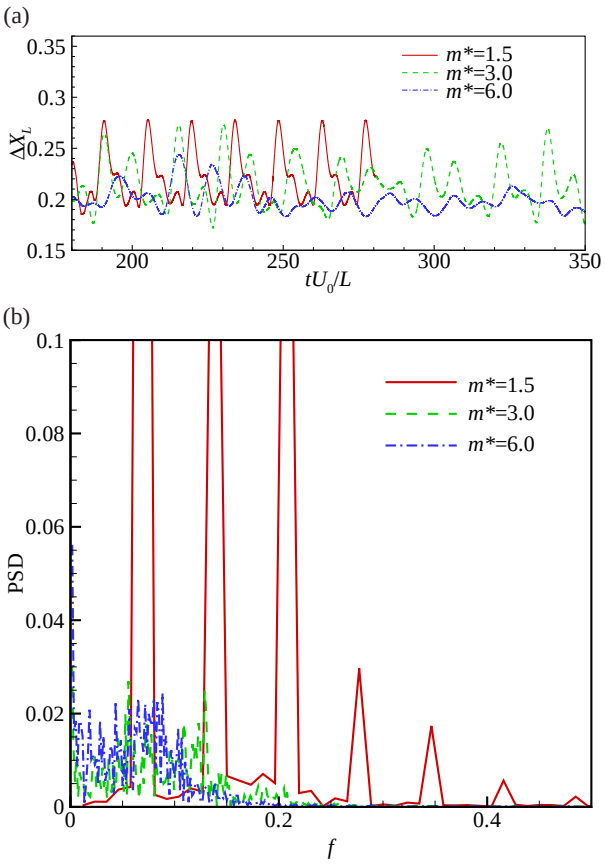

Figure 3: Mass ratio effects: (a) ΔX_L and (b) PSD.

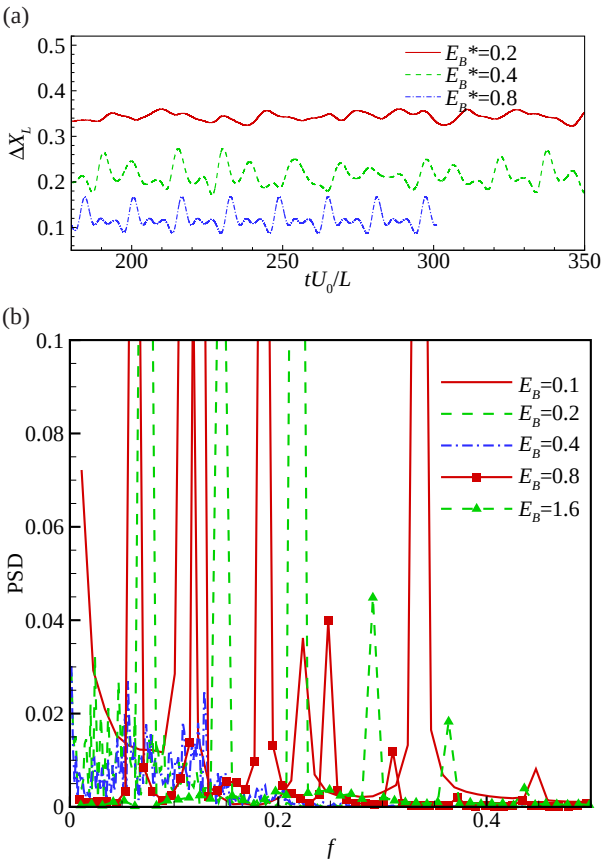

Figure 4: Bending rigidity effects: (a) ΔX_L and (b) PSD.

for $E_B^* = 0.8$ and $N = 5$ for $E_B^* = 1.6$. Therefore, the structure dynamics can be considered as periodic motion with period-doubling events. This observation is caused by the interplay of the structure vibration and the vortex dynamics in the wake.

Conclusions

In this paper, an immersed boundary method has been used to study the fluid–structure interaction of a flexible plate vertically fixed in a laminar boundary layer over a rigid wall by considering the effects of the Reynolds number, structure-to-fluid mass ratio and bending rigidity. We have discussed the vibrations and frequencies of the plate, finding that the plate exhibits much richer phenomena compared to flag vibrations in uniform flows as both convective and absolute instabilities are encountered in this situation, while in traditional flow-induced vibration of a flag, only convective instability is involved. In addition, varying the bending rigidity of the plate has potential to change the frequencies.

Acknowledgements

Dr. F.-B. Tian is the recipient of an Australian Research Council Discovery Early Career Researcher Award (project number DE160101098). This work was partly supported by the Silverstar grant, UNSW Canberra, and was partly undertaken on the NCI National Facility in Canberra, Australia, which is supported by the Australian Commonwealth Government.

References

[1] Alben, S., The flapping-flag instability as a nonlinear eigenvalue problem, *Phys. Fluids*, **20**, 2008, 104106.

[2] Alben, S., Wake–mediated synchronization and drafting in coupled flags, *J. Fluid Mech.*, **641**, 2009, 489–496.

[3] Alben, S. and Shelley, M., Flapping states of a flag in an inviscid fluid: bistability and the transition to chaos, *Phys. Rev. Lett.*, **100**, 2008, 074301.

[4] Argentina, M. and Mahadevan, L., Fluid-flow-induced flutter of a flag, *Proc. Natl. Acad. Sci. U.S.A.*, **102**, 2005, 1829–1834.

[5] Connell, B. S. H. and Yue, D. K. P., Flapping dynamics of a flag in a uniform stream, *J. Fluid Mech.*, **581**, 2007, 33–67.

[6] Dai, L., He, G. and Zhang, X., Self-propelled swimming of a flexible plunging foil near a solid wall, *Bioinspir. Biomim.*, **11**, 2016, 046005.

[7] Eloy, C., Lagrange, R., Souilliez, C. and Schouveiler, L., Aeroelastic instability of cantilevered flexible plates in uniform flow, *J. Fluid Mech.*, **611**, 2008, 97–106.

[8] Eloy, C., Souilliez, C. and Schouveiler, L., Flutter of a rectangular plate, *J. Fluids Struct.*, **23**, 2007, 904–919.

[9] Huang, L., Flutter of cantilevered plates, *J. Fluids Struct.*, **9**, 1995, 127–147.

[10] Huang, W. X., Shin, S. J. and Sung, H. J., Simulation of flexible filaments in a uniform flow by the immersed boundary method, *J. Comput. Phys.*, **226**, 2007, 2206–2228.

[11] Liu, Y., Lei, C. and Patterson, J. C., Plume separation from an adiabatic horizontal thin fin placed at different heights on the sidewall of a differentially heated cavity, *Int. Commun. Heat Mass Transf.*, **61**, 2015, 162–169.

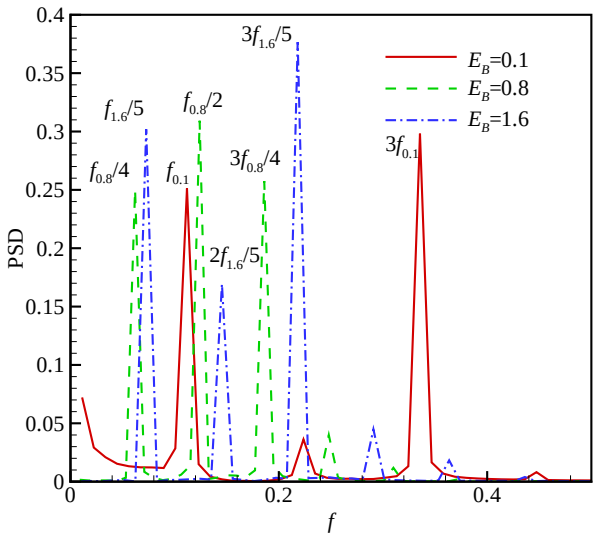

Figure 5: Frequency comparison between small and large bending rigidities.

[12] Michelin, S. and Llewellyn Smith, S. G., Linear stability analysis of coupled parallel flexible plates in an axial flow, *J. Fluids Struct.*, **25**, 2009, 1136–1157.

[13] Sader, J. E., Cossé, J., Kim, D., Fan, B. and Gharib, M., Large-amplitude flapping of an inverted flag in a uniform steady flow a vortex-induced vibration, *J. Fluid Mech.*, **793**, 2016, 524–555.

[14] Schouveiler, L. and Eloy, C., Coupled flutter of parallel plates, *Phys. Fluids*, **21**, 2009, 081703.

[15] Shahzad, A., Tian, F. B., Young, J. and Lai, J. C., Effects of flexibility on the hovering performance of flapping wings with different shapes and aspect ratios, *J. Fluids Struct.*, **81**, 2018, 69–96.

[16] Shelley, M., Vandenberghe, N. and Zhang, J., Heavy flags undergo spontaneous oscillations in flowing water, *Phys. Rev. Lett.*, **94**, 2005, 094302.

[17] Tian, F. B., Role of mass on the stability of flag/flags in uniform flow, *Appl. Phys. Lett.*, **103**, 2013, 034101.

[18] Tian, F. B., FSI modeling with the DSD/SST method for the fluid and finite difference method for the structure, *Comput. Mech.*, **54**, 2014, 581–589.

[19] Tian, F. B., Dai, H., Luo, H., Doyle, J. F. and Rousseau, B., Fluid–structure interaction involving large deformations: 3D simulations and applications to biological systems, *J. Comput. Phys.*, **258**, 2014, 451–469.

[20] Tian, F. B., Lu, X. Y. and Luo, H., Onset of instability of a flag in uniform flow, *Theor. Appl. Mech. Lett.*, **2**, 2012, 022005.

[21] Tian, F. B., Luo, H., Song, J. and Lu, X. Y., Force production and asymmetric deformation of a flexible flapping wing in forward flight, *J. Fluids Struct.*, **36**, 2013, 149–161.

[22] Tian, F. B., Luo, H., Zhu, L., Liao, J. C. and Lu, X. Y., An immersed boundary-lattice Boltzmann method for elastic boundaries with mass, *J. Comput. Phys.*, **230**, 2011, 7266–7283.

[23] Tian, F. B., Luo, H., Zhu, L. and Lu, X. Y., Coupling modes of three filaments in side-by-side arrangement, *Phys. Fluids*, **23**, 2011, 111903.

[24] Tian, F. B., Young, J. and Lai, J. C. S., Improving power-extraction efficiency of a flapping plate: From passive deformation to active control, *J. Fluids Struct.*, **51**, 2014, 384–392.

[25] Xu, F., Patterson, J. C. and Lei, C., Transient natural convection flows around a thin fin on the sidewall of a differentially heated cavity, *J. Fluid Mech.*, **639**, 2009, 261–290.

[26] Zhang, J., Childress, S., Libchaber, A. and Shelley, M., Flexible filaments in a flowing soap film as a model for one-dimensional flags in a two-dimensional wind, *Nature*, **408**, 2000, 835–839.

[27] Zhao, Y., Lei, C. and Patterson, J. C., Resonance of the thermal boundary layer adjacent to an isothermally heated vertical surface, *J. Fluid Mech.*, **724**, 2013, 305–336.

[28] Zhu, L., He, G., Wang, S., Miller, L., Zhang, X., You, Q. and Fang, S., An immersed boundary method by the lattice Boltzmann approach in three dimensions with application, *Comput. Math. Appl.*, **61**, 2011, 3506–3518.

[29] Zhu, L. and Peskin, C. S., Simulation of a flapping flexible filament in a flowing soap film by the immersed boundary method, *J. Comput. Phys.*, **179**, 2002, 452–468.